Oncogene (2009) 28, 1121–1131

www.nature.com/onc

ORIGINAL ARTICLE

# EGR-1 forms a complex with YAP-1 and upregulates Bax expression in irradiated prostate carcinoma cells

M Zagurovskaya[1,7], MM Shareef[1,7,8], A Das[2,7], A Reeves[1], S Gupta[1,8], M Sudol[1], MT Bedford[3], J Prichard[4], M Mohiuddin[5] and MM Ahmed[1,6,8]

[1]*Weis Center for Research, Geisinger Clinic, Danville, PA, USA;* [2]*Department of Internal Medicine, Virginia Commonwealth University, Richmond, VA, USA;* [3]*Department of Carcinogenesis, M.D. Anderson Cancer Center, University of Texas, Smithville, TX, USA;* [4]*Department of Pathology, Geisinger Clinic, Danville, PA, USA;* [5]*Geisinger-Fox Chase Cancer Center, Geisinger Clinic, Wilkes-Barre, PA, USA and* [6]*Department of Radiation Oncology, Fox Chase Cancer Center, Philadelphia, PA, USA*

**In this study, we investigated the functional role of early growth response-1 (*Egr1* gene) in the regulation of radiation-induced clonogenic inhibition and apoptosis in p53 wild-type and mutant prostate cancer cells 22Rv1 and DU145, respectively. 22Rv1 cells were more sensitive to irradiation compared with DU145 cells, and the sensitivity was enhanced by overexpression of EGR-1 in both cells. Dominant-negative EGR-1 mutant (dnEGR-1) or repressor of EGR-1, NGFIA binding protein 1 (NAB1), increased radioresistance of these cells. Significant activation of caspases 3 and 9 and Bcl2-associated X (Bax) with increased poly(ADP-ribose) polymerase (PARP) cleavage and cytochrome *c* release was observed in radiation-exposed EGR-1 overexpressing cells. Gel shift analysis and chloramphenicol acetyl transferase (CAT) reporter assays indicate that EGR-1 transactivates the promoter of the Bax gene. Interaction of EGR-1 and Yes kinase-associated protein 1 (YAP-1) through the WW domain of YAP-1 enhances the transcriptional activity of EGR-1 on the Bax promoter as shown by chromatin immunoprecipitation and reporter assays. Irradiation of PC3 cell xenografts that were treated with adenoviral EGR-1 showed significant regression in tumor volume. These findings establish the radiation-induced pro-apoptotic action of EGR-1, in a p53-independent manner, by directly transactivating Bax, and prove that alters the B-cell CLL/lymphoma 2 (Bcl-2)/Bax ratio as one of the mechanisms resulting in significant activation of caspases, leading to cell death through the novel interaction of EGR-1 with YAP-1.**
*Oncogene* (2009) **28,** 1121–1131; doi:10.1038/onc.2008.461; published online 12 January 2009

**Keywords:** EGR-1; YAP-1; Bax; prostate cancer; radiation

Correspondence: Dr MM Ahmed, Department of Radiation Oncology, Sylvester Comprehensive Cancer Center, Miller School of Medicine, University of Miami, Miami, FL 33136, USA.
E-mail: amansoor@med.miami.edu
[7]These authors contributed equally to this work.
[8]Current address: Department of Radiation Oncology, Sylvester Comprehensive Cancer Center, University of Miami, FL 33136, USA
Received 18 March 2008; revised 31 October 2008; accepted 13 November 2008; published online 12 January 2009

## Introduction

Loss of the apoptotic response to ionizing irradiation (IR) by overexpression of pro-survival or downregulation of pro-apoptotic genes has been linked to a radioresistant phenotype (Kyprianou, 1994). In this study, we selected the *Egr*-1 gene to understand its role in radiation resistance, because (a) upon orchiectomy *Egr*-1 was rapidly induced, leading to apoptosis of androgen-dependent prostate cells (Buttyan *et al*., 1988; Day *et al*., 1993); (b) IR upregulates EGR-1 expression (Datta *et al*., 1992); and (c) EGR-1 protein upregulates pro-apoptotic gene expression (Ahmed *et al*., 1997; Nair *et al*., 1997; Das *et al*., 2001).

Alterations in p53 function has been attributed to increased radioresistance (Lee and Bernstein, 1993). EGR-1 protein upregulates p53 in response to thapsigargin-induced apoptotic stimuli (Nair *et al*., 1997). Expression of dominant-negative EGR-1 mutant (dnEGR-1) in melanoma cells (wt p53) caused radio resistance (Ahmed *et al*., 1996). Despite the absence of p53 protein, the cells overexpressing EGR-1 protein were sensitive to IR, which was associated with upregulation of tumor necrosis factor-α protein through EGR-1-mediated transactivation (Ahmed *et al*., 1997). In addition, *Egr*-1$^{-/-}$ mouse embryonic fibroblast cells were highly radioresistant as compared with *Egr*-1$^{+/-}$ mouse embryonic fibroblast cells, where the radiation-induced pro-apoptotic function of EGR-1 was solely mediated by the target genes such as p53 and retinoblastoma (Das *et al*., 2001). Thus, EGR-1 plays an important role in the regulation of radiation-induced apoptosis through p53, retinoblastoma and tumor necrosis factor-α target genes.

Yes kinase-associated protein-1 (YAP-1), a transcriptional co-activator of p73, is a 65-kDa protein, also referred to as YAP-65. YAP-1, originally identified as an interaction partner of Src family tyrosine kinase, Yes (Sudol, 1994), contains one WW domain, a PDZ-interacting motif, SH3-binding motif and a coiled-coil domain. A differentially spliced isoform of YAP-1, with two WW domains known as YAP-2 also exists (Sudol *et al*., 1995). Phosphorylation of YAP by Akt or Lats1 attenuates the p73-mediated transcriptional activity and

apoptosis (Basu *et al*., 2003; Oka *et al*., 2008). Whether EGR-1, like p73, is regulated through a similar interaction is not known.

Understanding the role played by radiation-induced EGR-1 in apoptosis could be crucial in designing therapy for prostate tumor control. We investigated the function of *Egr*-1 in radiation-induced apoptosis using wt-p53 (22Rv1), mutant p53 (DU145), P53 null (PC3) prostate cancer cell line and PC3 xenografts in mice. Overexpression of EGR-1 protein transactivates Bax causing an imbalance in the Bcl-2/Bax protein ratio and rendering enhanced susceptibility to radiation-induced apoptosis. Regulation of Bax expression by the interaction of EGR-1 with YAP-1 is suggestive of a novel mode of regulation of EGR-1 targets that could play a crucial role in the apoptosis mediated by EGR-1.

## Results

*Overexpression of EGR-1 increases sensitivity to radiation-induced clonogenic inhibition and apoptosis*

Radiation-induced activity of EGR-1 was minimal in both DU145 cells (3%) and 22Rv1 (8%) cells. Overexpression of EGR-1 by transfection or adenoviral infection in DU145 and 22Rv1 cells, respectively, significantly induced the EBS (EGR-1 binding site)-CAT activity in the untreated and irradiated cells (7.5- and 10.7-fold (DU145 cells), and 4- and 4.5-fold (22Rv1 cells) (Figure 1a). DU145 and 22Rv1 cells show induction of EGR-1 protein by 5 Gy radiation as early as 15–30 min. The protein expression correlated with the EBS-CAT activity with more activity in 22Rv1 cells than in DU145 cells (Supplementary Figure 1a, Figure 1a). Although EGR-1 expression is more in 22Rv1 cells compared with DU145 cells, the functional activity is not significantly different (Figure 1a, Supplementary Figure 1a and c). The 22Rv1 cells were found to be more radiosensitive compared with the DU145 cells by clonogenic assay (Supplementary Figure 1b). As basal EGR-1 transactivation function of EGR-1 was low in DU145 cells (Supplementary Figure 1c), ectopic overexpression of EGR-1 was achieved by stable transfections with CMV EGR-1 (a 2.5-fold increase in protein expression, Supplementary Figure 2a). Further, infection with Ad-EGR-1 in 22Rv1 cells causing a nine-fold increase in EGR-1 protein expression (Supplementary Figure 2b) was also used. Overexpression of NGFIA binding protein 1 (NAB1), an EGR-1 repressor, reduced the endogenous EGR-1 in 22Rv1 cells, as EGR-1 regulates it own transcription (Supplementary Figure 2b). Overexpression or repression of EGR-1, respectively, led to an increased or decreased EBS-CAT and EGR-1-binding activities (electrophoreticmobility shift assay) (Supplementary Figure 1c and 2c).

Using colony-forming assay, $SF_2$ and $D_0$ values of irradiated DU145/Vector cells were 0.609 and 400 cGy, respectively (Figure 1b). On the other hand, the $SF_2$ value for dnEGR-1 was 0.66 with the $D_0$ value of 509 cGy, suggesting that the cells transfected with the dnEGR-1 were more radioresistant ($P<0.001$). The $SF_2$ value for CMV-EGR-1 was 0.34 with the $D_0$ value of 164 cGy, suggesting enhanced radiation sensitivity ($P<0.0001$) with EGR-1 overexpression (Figure 1).

Similarly, terminal deoxynucleotidyl transferase nick end labeling (TUNEL) and flow cytometric analysis indicated that DU145/dnEGR-1 cells were resistant ($P<0.001$) and DU145/CMV-EGR-1 cells were significantly sensitive ($P<0.0001$) to IR-inducible apoptosis (Supplementary Figure 3a and b).

In 22Rv1 cells, the $SF_2$ value of cells infected with Ad-green fluorescent protein (Ad-GFP) was 0.45 with a $D_0$ value of 270 cGy (Figure 1c). On the other hand, the $SF_2$ value for Ad-NAB1-infected cells was 0.63 with the $D_0$ value of 375 cGy, suggesting that the cells infected with the EGR-1 repressor NAB1, were more radioresistant ($P<0.001$). Overexpression of EGR-1 (by Ad-EGR-1) showed an $SF_2$ value of 0.29 with the $D_0$ value of 151 cGy, suggesting enhanced radiosensitivity ($P<0.0001$). TUNEL assay and flow cytometric analysis also indicated that Ad-NAB1-infected cells were radioresistant ($P<0.001$) and Ad-EGR-1-infected cells were significantly more radiosensitive ($P<0.0001$) (Supplementary Figure 3c and d). Together these findings suggest that EGR-1 is required for IR-induced apoptosis, and overexpressed EGR-1 potentiates the effects of IR.

*EGR-1 induces the expression of BAX*

On the basis of above results, we hypothesized that the pro-apoptotic proteins might have been altered by EGR-1. A significant upregulation of Bax protein in both untreated and irradiated DU145/CMV-EGR-1 cells with a slight reduction in the Bcl-2 protein level in EGR-1-overexpressing cells was observed (Figure 2a). Significant induction of Bax mRNA was observed in cells overexpressing EGR-1 as compared with that of cells transfected with dnEGR-1 or vector alone in both the untreated and irradiated cells (Figure 2b). Similar results were obtained with 22Rv1 cells, suggesting a role for EGR-1 in regulating the expression of Bax (Figure 2c). In order to show that expression of EGR-1 leads to activation of Bax, oligomerization and activation of Bax were performed in 22Rv1 cells. Overexpression and/or irradiation lead to increased Bax oligomerization, suggesting an activation of Bax without any change in the levels of β-actin used as an internal control (Figure 2d). As Bax affects mitochondrial permeability, causing the release of cytochrome *c*, leading to caspase activation (Tsujimoto, 1998), specific activity of caspases 3 and 9 were analyzed at different time intervals after radiation. DU145 cells transfected with EGR-1 showed elevated caspases 3 and 9 activity (Supplementary Figure 4a and b). Western blot analysis of inactive form of caspase 3 shows a decrease with time in irradiated cells transfected with EGR-1. Pro-apoptotic events mediated by EGR-1 are further reflected in the cleavage of 116-kDa poly(ADP-ribose) polymerase (PARP) (Supplementary Figure 4c). Overexpression of EGR-1 by Ad-EGR-1 caused an increase in the release

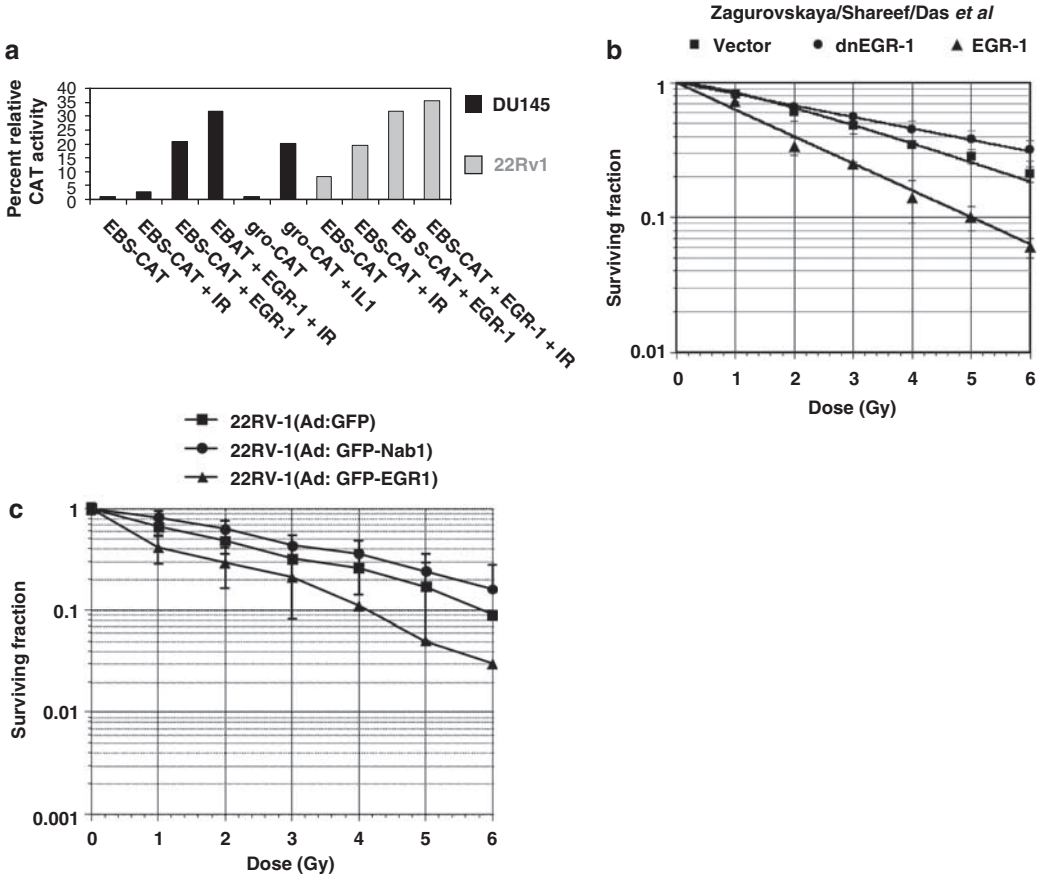


**Figure 1** Ectopic early growth response-1 (EGR-1) expression radiosensitizes prostate carcinoma cells. (**a**) Overexpression of EGR-1 in DU145 and 22Rv1 cells induces EBS-CAT reporter activity that is further enhanced by radiation. DU145 and 22Rv1 cells were transiently transfected with EBS-CAT reporter activity. Protein extracts from these cells were used for CAT assay. Transfections with gro-CAT or gro-CAT plus IL1 were used as positive controls. Relative percent CAT activity is represented as histograms. (**b**) Dose–response curves of DU145 cells stably transfected with vector alone, dnEGR-1 or EGR-1 as assessed by clonogenic inhibition assay. $SF_2$ value for DU145 cells transfected with vector alone was found to be 0.609 with a $D_0$ value of 400 cGy. $SF_2$ value for dominant-negative EGR-1 mutant (dnEGR-1)-transfected cells was 0.66 with a $D_0$ value of 509 cGy. $SF_2$ value for EGR-1 transfected cells was 0.34 with a $D_0$ value of 164 cGy. (**c**) Dose–response curves of 22Rv1 cells infected with Ad-GFP, Ad-NAB1 or Ad-EGR-1 as assessed by clonogenic inhibition assay. $SF_2$ value for 22Rv1 cells infected with Ad-GFP was found to be 0.45 with a $D_0$ value of 270 cGy. $SF_2$ value for Ad-NAB1-infected cells was 0.63 with a $D_0$ value of 375 cGy. $SF_2$ value for Ad-EGR-1-infected cells was 0.29 with a $D_0$ value of 151 cGy.

of cytochrome *c* levels in cytosolic versus mitochondrial fractions in untreated and irradiated cells. In contrast, overexpression of NAB1 caused a decreased cytochrome *c* release (Supplementary Figure 4d). Promoter analysis of Bax gene indicated two putative overlapping Egr-1-binding sites from −21 to −13 (GCGGCGGCG) and from −15 to −7 (GCGGGAGCG) with one base variation when compared with the consensus Egr-1-binding site (Figure 3a). To ascertain whether these sites could bind to EGR-1 protein, we performed electrophoreticmobility shift assay and CAT reporter assays (Figure 3a). Electrophoreticmobility shift assay indicated that radio-labeled EGR-1 consensus oligo probe (from Bax promoter sequence) was competitively reduced with cold probe. Furthermore, EGR-1 binding to probe was reduced in supershift assays (Figure 3b).

DU145 cells showed a modest background level of CAT activity (Figure 3c) that increased significantly with EGR-1 overexpression. On the other hand, CAT activity induced by EGR-1 was reduced by dnEGR-1, suggesting that EGR-1 transactivates, and the dnEGR-1 transrepresses, the Bax promoter. EBS-deleted pBax-CAT construct showed attenuation of basal expression driven by the promoter, and ectopically expressed EGR-1 caused no induction of CAT activity (Figure 3c). Similarly, overexpression of EGR-1 significantly induced CAT activity in 22Rv1 cells. On the other hand, significant reduction in CAT activity was observed with NAB1. The pΔBax-CAT vector could not be induced with Ad-EGR-1 (Figure 3d). Thus, these findings suggest that EGR-1 transactivates the Bax through the EGR-1-binding site in its promoter.

### *WW domain-binding motif PPxY regulates the transactivation function of EGR-1*

p300/CBP proteins bind to transcription factors through their cysteine- and histidine-rich (C/H) domains to form active transcriptional complexes (Kalkhoven, 2004). A potential acetylation of KDKK motif in EGR-1 is

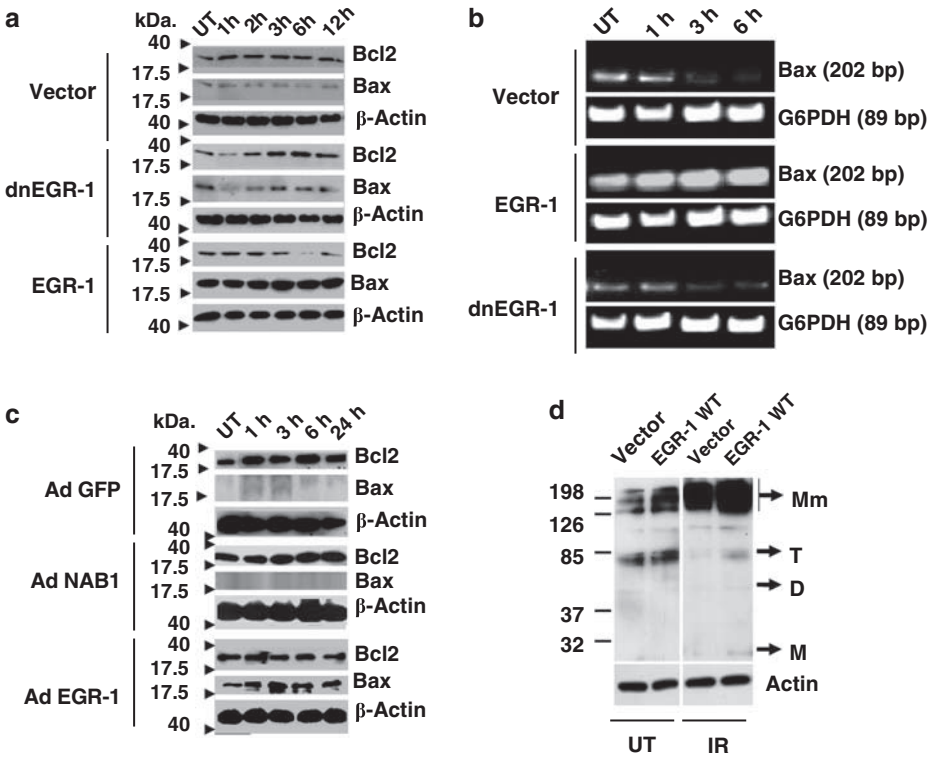


**Figure 2** Ectopic early growth response-1 (EGR-1) induces the expression of Bax protein in prostate carcinoma cells. (**a**) Western analysis. DU145 cells transfected with vector, dnEGR-1 or EGR-1 were either left untreated (UT) or treated with 5 Gy X-ray irradiation. Protein extracts were prepared from these cells after 1, 2, 3, 6 and 12 h post irradiation. Blots of these proteins were probed for expressions of Bax, Bcl2 and β-actin. (**b**) Reverse transcriptase-PCR analysis. DU145 cells transfected with vector, dnEGR-1 or EGR-1 were either untreated or treated with 5 Gy X-ray irradiation. Total RNA was prepared from these cells 1, 3 and 6 h post irradiation. The mRNA levels of Bax and G6PDH as a function of EGR-1 activity are shown. (**c**) Western analysis. 22Rv1 cells infected with Ad-GFP, Ad-NAB1 or Ad-EGR-1 were either left untreated (UT) or treated with 5 Gy X-ray irradiation. Protein extracts were prepared from these cells 1, 3, 6 and 24 h post irradiation. Blots of these proteins were probed for expressions of Bax, Bcl2 and β-actin. (**d**) Oligomerization of BAX. PC3 cells transfected with vector or EGR-1 were either untreated or irradiated with 5 Gy radiation and the cells were crosslinked with bis-(sulfosuccinimidyl) suberate and disuccinimidyl suberate (Pierce, Rockford, IL, USA) as per the method of Antonsson *et al.* (2001). Whole lysates were prepared in RIPA buffer and separated by non-reducing SDS–PAGE and blotted onto polyvinylidene fluoride (PVDF) membrane. The membrane was probed using anti-Bax antibody.

required for its interaction with p300 (Matheny *et al*., 1994). YAP-1, a WW domain-containing protein, by binding to p73 recruits p300 to p73 target genes, leading to the induction of these genes (Basu *et al*., 2003). We reasoned that a similar mechanism might be responsible for recruitment of YAP-1 and p300 to the EGR-1-binding sites. Analysis of the primary sequence of EGR-1 revealed the presence of a WW domain-interacting PPxY motif ($^{235}$YPPPAY$^{240}$) in EGR-1 (Figure 4a). To find out whether the PPxY motif is critical in the activation of EGR-1, EGR-1 (Y240A) mutant was constructed. Aromatic amino acid residue (Y235) present at the N terminus of the PPxY motifs, which is a crucial determinant of the WW domain-binding activity, was also mutated (Macias *et al*., 2002). Both the mutations (Y235,240A) lead to a decrease in the EBS-CAT reporter activity in PC3 cells, suggesting that this motif is required for maximal transcriptional activation of EGR-1 (Figure 4b). Approximately 18 and 39% reduction in EGR-1 activity was observed with EGR-1 (Y240A) and EGR-1 (Y235,240A) mutations, respectively. An average of 24 and 38% reduction of activity was observed in irradiated cells (Figure 4b). Similar reduction in the EBS-GFP-positive cells was observed in PC3 cells transfected with EGR-1 (Y240A) (48.5%) and EGR-1 (Y235,240A) (45.5%) mutations (Figure 4c). Dramatic reduction in the BAX-CAT reporter activity was observed in 22Rv1 cells transfected with EGR-1 (Y240A) (76%) and EGR-1 (Y235,240A) (86%) mutations (Figure 4d).

### *YAP-1 binding to EGR-1 is required for the clonogenic cell death mediated by EGR-1*

PC3 cells stably transfected with pCB6 EGR-1 or EGR-1 mutants (EGR-1 Y240A; EGR-1 Y235,240A) were used for clonogenic assay. EGR-1 was found to decrease cell survival with $SF_2$ value of $0.154 \pm 0.0018$ when compared with vector alone ($0.292 \pm 0.0049$). This was reversed when YAP-1-binding mutants of EGR-1 were used. EGR-1 Y240A-transfected cells showed $SF_2$ value of $0.21 \pm 0.008$. Mutation of EGR-1 at Y235,240A was more effective as the cells transfected with EGR-1 Y235,240A shoed $SF_2$ value of $0.25 \pm 0.008$ (Figure 4e).

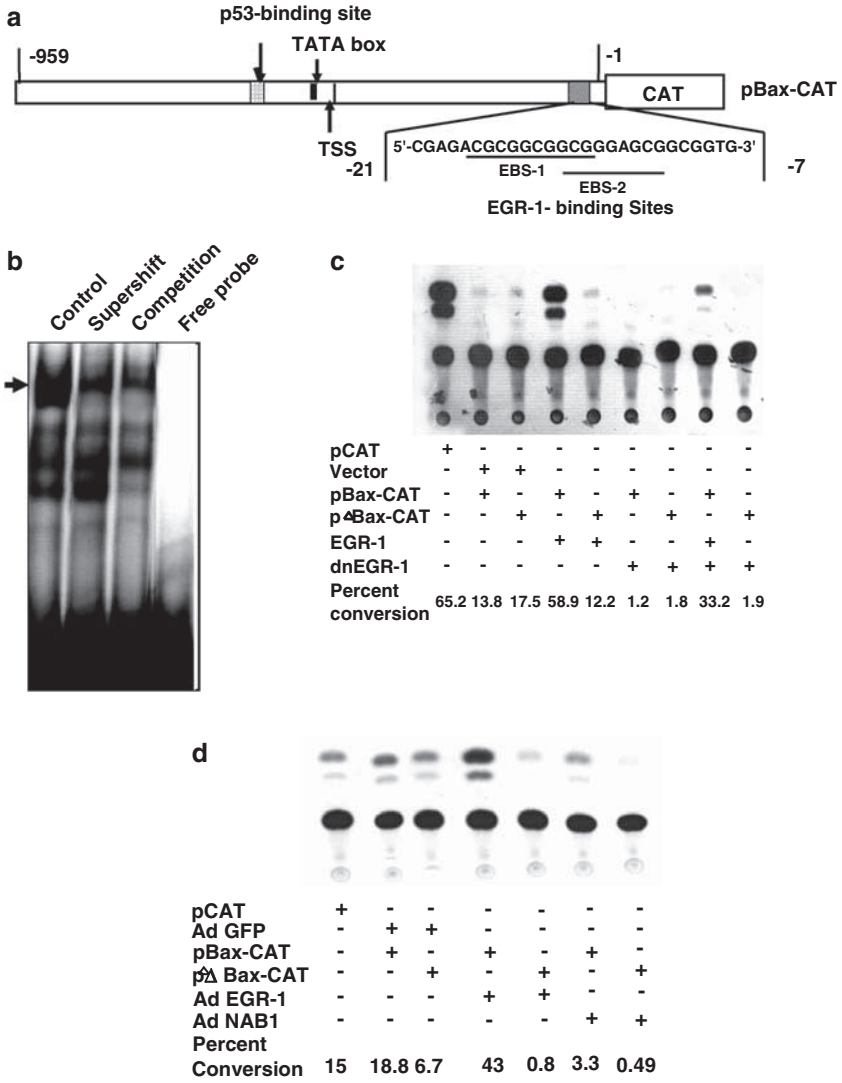


**Figure 3** Bax is a direct target of early growth response-1 (EGR-1). (**a**) Diagrammatic representation of Bax promoter in a reporter vector. Bax promoter used in our studies shows binding sites for EGR-1 (EBS1 and EBS2). TSS indicates transcription start site. TATA box and p53 binding sites are shown. Reporter construct deleted for EGR-1-binding sites is represented by sequence between −823 and −56. (**b**) EMSA showing binding of EGR-1 to BAX promoter oligos. Nuclear extracts from DU145 cells stably overexpressing EGR-1 were used. The arrow indicates bound complex. Competition suggests competition of hot probe by the cold probe. Supershift was performed by incubating the EGR-1 probe mixture with antibody against EGR-1. Control shows shift assay with probe and protein complex alone. (**c**) CAT reporter assay in DU145 cells. DU145 cells were transiently transfected with different combinations of plasmid outlined in the figure. CAT activity in each transfection was reported as percent conversion in the figure. (**d**) CAT reporter assay in 22Rv1 cells. 22Rv1 cells infected with Ad-GFP, Ad-NAB1 or Ad-EGR-1 were transiently transfected with different combinations of plasmid outlined in the figure. CAT activity in each transfection was reported as percent conversion in the figure.

YAP-1 siRNA caused pronounced cell survival in both untreated and irradiated PC3 cells as measured by real-time cell electronic signal system (data not shown).

*Protein array of WW, SH3 and Tudor domains using PPxY motif identifies YAP-1 as the protein interacting with EGR-1*

Owing to a significant role of PPxY motifs in EGR-1 activity, we reasoned that EGR-1 might be interacting with a WW domain-containing protein. Glutathione-*S*-transferase (GST) fusion proteins harboring the listed WW, SH3 and Tudor domains were arrayed (Espejo and Bedford, 2004). Biotinylated peptide motifs encompassing the PPxY motifs in EGR-1 or with mutants were used to identify the proteins interacting with these motifs. The wild-type peptides showed strong interaction with WW domain of YAP and this interaction was weak or absent with the mutant peptides. Interaction of the biotinylated peptides with the WW domain-containing proteins such as Itck and RSP II were also detected. Other domain-containing proteins including the SH3

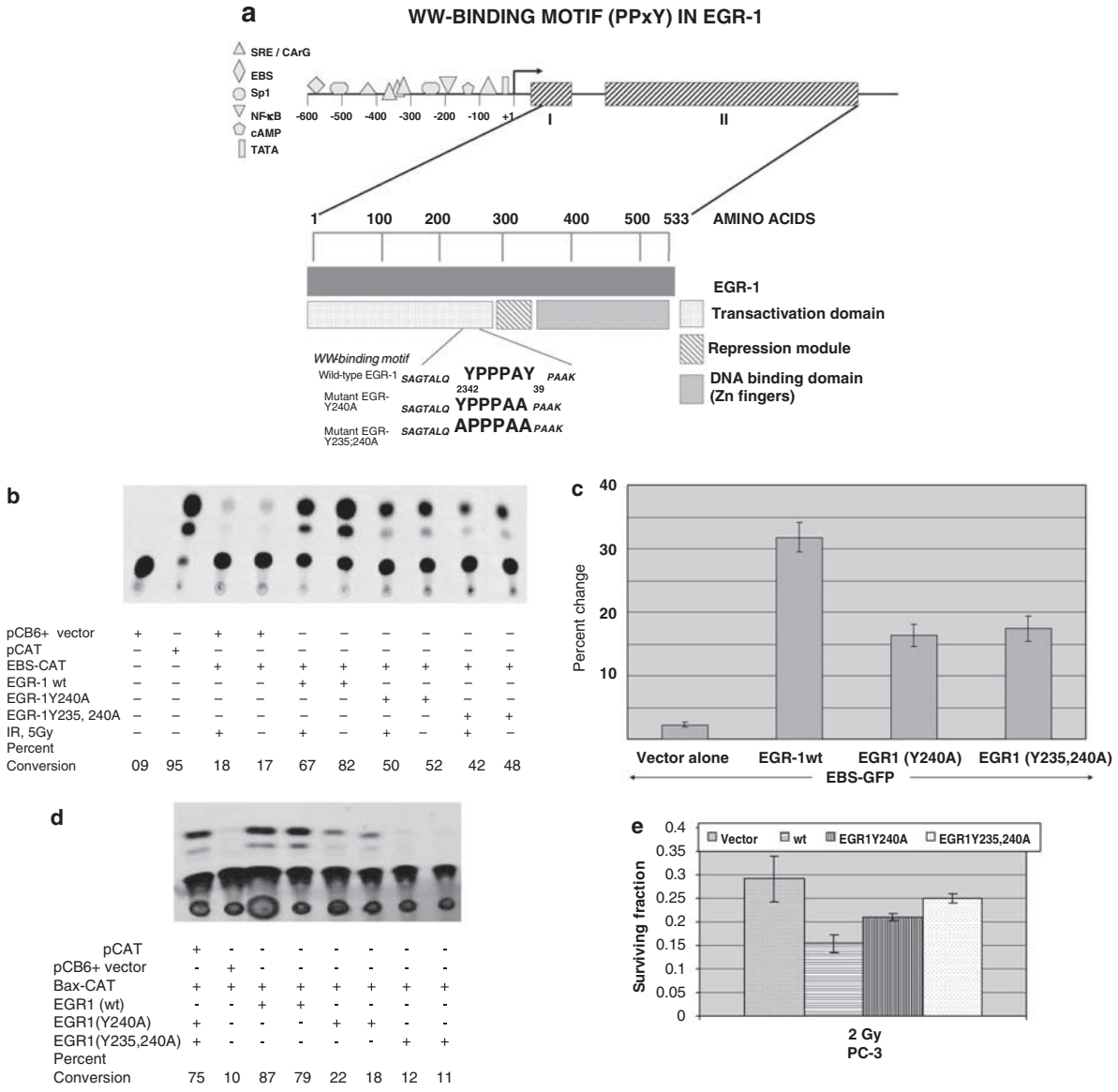


**Figure 4** WW domain-binding motif PPxY is important regulator of early growth response-1 (EGR-1) activity. (**a**) Diagrammatic representation of PPxY motif in EGR-1. PPxY motif in EGR-1 is present in the repression module II of EGR-1. Residues 237–240 represent the PPxY motif (PPAY). Aromatic residues at the N terminus are known to have an effect on binding. Therefore, the mutants that were generated include EGR-1 Y240A and EGR-1 Y235-240A. (**b** and **c**) PPxY motifs are essential for the transactivation function of EGR-1 in PC3 cells. Both the EGR-1 mutants EGR-1 Y240A and EGR-1 Y235-240A were found to possess reduced activity as assessed by EBS-CAT (**b**) as well as EBS-GFP (**c**) reporter activity. (**d**) PPxY motifs are essential for the activity of EGR-1 in 22Rv1 cells. Both the EGR-1 mutants EGR-1 Y240A and EGR-1 Y235-240A were found to possess reduced activity as assessed by BAX-CAT reporter activity. (**e**) Yes kinase-associated protein 1 (YAP-1) binding to EGR-1 is required for the clonogenic cell death mediated by EGR-1. Colony-forming assay indicates that YAP-1 binding to EGR-1 through PPxY motif is required for EGR-1-mediated clonogenic cell death. EGR-1 (wild type) significantly reduces cell survival, which is reversed with EGR-1 mutant lacking YAP-1-binding motifs.

domain or Tudor domain-containing fusion proteins did not show any interaction (Figure 5a).

*EGR-1 interacts with YAP-1 through its PPxY motif*

Reciprocal immunoprecipitation was carried out to confirm the interaction between EGR-1 and YAP-1 seen in the above mentioned GST-fusion protein array. PC3 cell protein extracts were immunoprecipitated using anti-EGR-1 or anti-YAP-1 and the immunoprecipitates were probed with anti-YAP-1 or anti-EGR-1, respectively. Immunoprecipitation of YAP-1 with EGR-1 antibody and EGR-1 with YAP-1 antibody is suggestive of interaction of these proteins. Furthermore, a negative control, constituting an immunoprecipitation using nonspecific rabbit IgG, did not show the presence of either EGR-1 or YAP-1 (Figure 5b). To show that these proteins are engaged on the BAX promoter as a

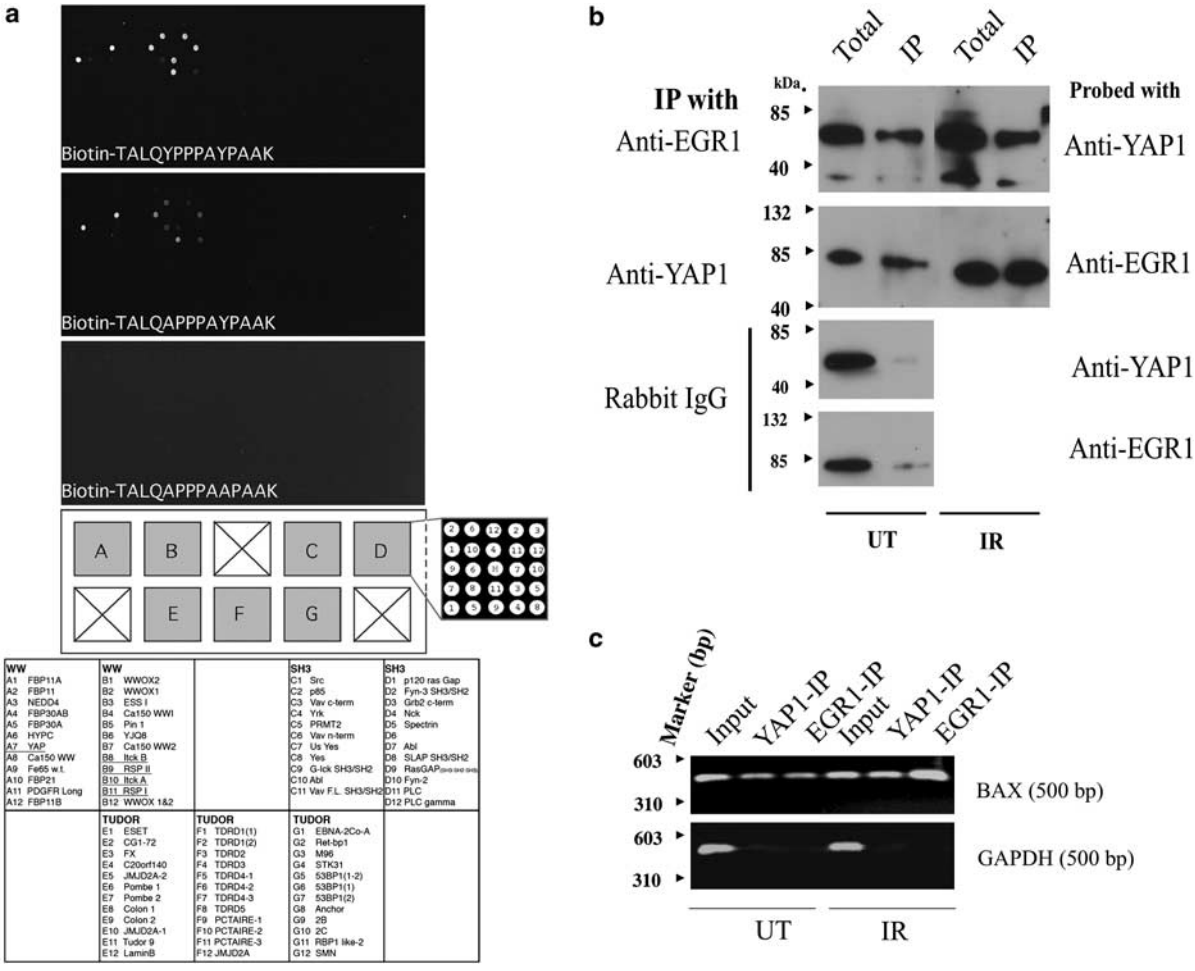


**Figure 5** Early growth response-1 (EGR-1) interacts with Yes kinase-associated protein 1 (YAP-1) through WW domain-interacting PPxY motif. (**a**) WW protein array detects YAP-1 as binding partner of EGR-1. WW, SH3 and TUDOR domain-containing GFP fusion protein array was probed with biotinylated PPxY encompassing motif from the EGR-1 protein. This motif was either wild type or mutant with aromatic tyrosine residues mutated to alanine. WW protein, YAP-1, was found to interact with the PPxY motif from EGR-1. This interaction was reduced or absent in mutants. (**b**) EGR-1 interacts with YAP-1. Extracts from PC3 cells were reciprocally immunoprecipitated with both EGR-1 or YAP-1 antibodies and the presence of YAP-1 and EGR-1 proteins, respectively, in these precipitates was analyzed by Western immunoblot analysis. Results show specific interaction of EGR-1 with YAP-1. (**c**) EGR-1–YAP-1 complex is present at the BAX promoter. Chromatin immunoprecipitation showed enrichment of BAX promoter in both the EGR-1 and YAP-1 ChIPs in the untreated and as well as in the irradiated PC3 cells. Irradiated EGR-1 ChIP showed more enrichment compared with untreated sample. Lack of GAPDH enrichment in ChIPs suggests the specificity of the EGR-1/YAP-1 localization at the BAX promoter.

complex, chromatin immunoprecipitation was carried out using anti-EGR-1 and anti-YAP antibodies on a nucleoprotein extract. PCR amplified the BAX promoter using the DNA immunoprecipitated by these antibodies, indicating enrichment of BAX promoter but not the nonspecific GAPDH gene suggestive of specific interaction of EGR-1 and YAP-1 at the BAX promoter (Figure 5c).

*Radiation induces the regression of tumor volumes of PC-3 xenografts infected with Ad-EGR-1*

To find out whether our *in vitro* findings translate in animal models of prostate cancer, PC-3 xenografts developed in nude mice were exposed to different treatment regimens outlined in Materials and methods section. Tumors treated with Ad-EGR-1 plus radiation showed a significant regression in tumor volume compared with those treated with Ad-GFP or Ad-EGR-1 or Ad-GFP plus radiation or radiation alone. No significant differences were observed between untreated and Ad-GFP-infected tumors, suggesting that adenoviral infection alone cannot change tumor volume. Interestingly, infection with Ad-EGR-1 alone significantly increased tumor volume as compared with radiation alone or Ad-GFP plus radiation or Ad-EGR-1 plus radiation, suggesting that in the absence of radiation, EGR-1 might potentially act as a pro-survival protein (Figure 6).

Immunohistochemical analysis of the PC3 xenograft tissue sections showed induction of Bax with both radiation or, Ad-EGR-1 alone. Elevated levels of Bax

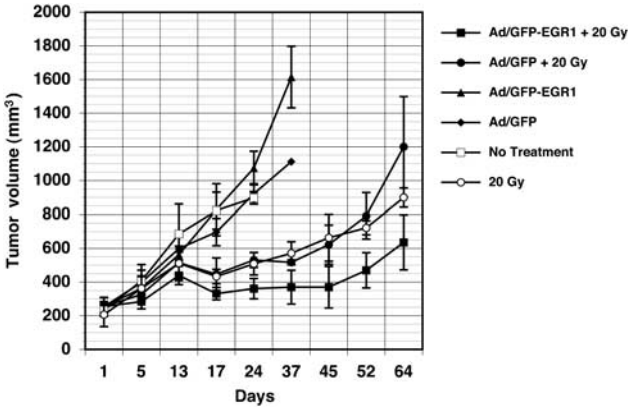


**Figure 6** Radiation sensitizes Ad-EGR-1-infected PC3 xenograft tumor cells leading to regression of tumor volume. Six different groups were used in these studies. Tumor volumes (represented by *Y* axis) were calculated at different time intervals (represented on the *X* axis) by the Attria and Weiss formula.

were found in Ad-EGR-1-infected tumors treated with radiation (Supplementary Figure 5). Thus, the tumor regression in response to combinatorial therapy involving ectopic EGR-1 and radiation could be mediated by Bax and the downstream apoptotic machinery.

## Discussion

Expression of EGR-1 positively correlates with the Gleason score, exclusively in prostate tumors (Eid *et al*., 1998). EGR-1 overexpression is correlated with the loss of its co-repressor NAB2 in primary prostate carcinoma causing elevated EGR-1 transcriptional activity (Abdulkadir *et al*., 2001a). Egr-1$^{-/-}$ TRAMP mice showed significant delay in prostate tumor formation compared with Egr-1$^{+/+}$ TRAMP mice, suggesting that the loss of EGR-1 failed to prevent tumor initiation, but delayed the progression of tumors (Abdulkadir *et al*., 2001b). On the contrary, EGR-1 can suppress growth when overexpressed or re-expressed in transformed cells. EGR-1 can induce apoptosis either by stimulating p53 activity or by IR (Ahmed *et al*., 1996, 1997), or PTEN expression (Virolle *et al*., 2001). Thus, it appears that EGR-1 can act as a tumor suppressor in some cells and as a growth stimulator in other cell types.

Regulation of p73 activity by acetylation of p73 and interaction with p300 resembles that of EGR-1 activity. YAP-1 functions as a co-activator of p73 (Basu *et al*., 2003). The role of YAP-1 in the process of tumorigenesis remains unclear. The unique feature of EGR-1 is its radio-inducibility, which would make it distinct from the p73. Zender *et al*. (2006) reported that YAP-1 is amplified in hepatocarcinoma and cooperates with Myc in transformation, implying that YAP-1 is an oncoprotein. Similarly, Dong *et al*. (2007) suggested that YAP-1 plays a role in size control mechanism in *Drosophila* and mammals . In contrast, other studies have shown that YAP-1 has antitumoral properties (Basu *et al*., 2003; Matallanas *et al*., 2007; Strano and Blandino, 2007). Furthermore, YAP-1 mRNA upregulation correlates with improved survival in breast cancer patients (Matallanas *et al*., 2007). Although it appears that YAP-1 may play a crucial role in the process of tumorigenesis, it may play an opposite role during radiation enabling the process of EGR-1-mediated apoptosis. EGR-1 mutants defective in binding to YAP-1 showed decrease in three BAX reporters tested (Figures 4b–d). We clearly show that the radiation-induced pro-apoptotic function of EGR-1 leading to clonogenic cell death is mediated through its interaction with YAP-1 (Figure 4e). Furthermore, physical interaction of EGR-1 and YAP-1 as shown by WW domain array, immunoprecipitation and ChIP (Figures 5b and c) suggests a role for EGR-1/YAP-1 complex in the regulation of BAX gene. We also found that Puma, a pro-apoptotic protein, was regulated by EGR-1/YAP-1 (Reeves A and Ahmed MM. EGR-1 mediated up-regulation PUMA is regulated by PPxY motif in the transactivation domain, unpublished results). This suggests that in addition to Bax activation, other mechanisms such as transactivation of Puma may mediate radiation-induced apoptotic function of EGR-1. In addition, marginal reductions in the levels of Bcl2 in cells expressing ectopic EGR-1 could be because of inhibition of nuclear factor-κB by binding of p65 subunit with EGR-1. The induction of Bax expression by EGR-1 with YAP-1 functioning as co-activator in irradiated cells, as shown in this study, is a significant step in understanding the pro-apoptotic mode of EGR-1 function during radiotherapy. Although overexpression of EGR-1 by adenoviral EGR-1 therapy increased in tumor volume, overexpression of EGR-1 with X-ray irradiation significantly regressed the tumor, suggesting that modulation of appropriate regulators of EGR-1, including YAP-1, by DNA-damaging agents such as IR could be useful in tumor control.

It was not clear how EGR-1 could mediate an apoptotic response in PC3 cells despite the lack of p53 protein in our earlier studies. Our present studies using two different prostate cancer cell lines, 22Rv1 (p53 wt) and DU145 (p53 mutant), show that the apoptotic function could be mediated directly by EGR-1 through the transcriptional upregulation of Bax mRNA, protein, and increased oligomerization and activation. It is likely that p73 with YAP-1 may also contribute to the transactivation of Bax. However, the radio-inducibility of EGR-1 makes it unique for mediating this function. Thus, it appears that IR primes EGR-1 for an important role in mediating apoptosis, independent of p53 function, through a novel mode of regulation by YAP-1

## Materials and methods

*Plasmid constructs*

The plasmid CMV-EGR-1 encoding full-length EGR-1 protein and dominant-negative EGR-1 was described earlier (Ahmed *et al*., 1997). EGR-1 mutants, EGR-1Y240A and EGR-1Y235,240A, were constructed by site-directed

mutagenesis. The reporter construct, EBS-CAT, contains three EGR-1 binding sites (CGCCCCCGC) placed in tandem upstream of a minimal c-fos promoter and CAT cDNA. The full-length Bax promoter region was PCR amplified from human genomic DNA, using sense primer (5′-TTTTTCTAGA CAGCACAGATTAGTTTCTGCCAC-3′, −959 to −937) and the antisense primer (5′-TTTTAAGCTTCACCGCCGCT CCCGCCGC-3′, −18 to −1) containing built-in sites (underlined) for *Xba*I and *Hin*dIII restriction sites, respectively. The Bax promoter without EGR-1-binding site was constructed using the sense primer (5′-TTTTTCTAGAATGCTT GAGTCTGGGAGTTCA-3′, −823 to −807) and the antisense primer (5′-TTTTAAGCTTCCCGGGTCACGTGAGAGC-3′ −73 to −56). The full-length Bax promoter (pBax-CAT) with or without EBS was cloned in the pG-CAT reporter plasmid. The EBS-GFP reporter plasmid was constructed by subcloning the promoter sequence into the *Ase*I–*Nhe*I cloning sites. Adenoviral construct expressing EGR-1 was a gift from Dr Jeffrey Milbrandt (Svaren *et al*., 2000).

*Cell Culture*
22Rv1 cells were grown in RPMI 1640 medium with 10% fetal bovine serum and 1% penicillin–streptomycin at 37 °C and 5% $CO_2$. DU145 (mutant p53) and PC-3 cells (p53 null) were grown in α-MEM and RPMI, respectively, supplemented with 10% fetal bovine serum and 1% penicillin–streptomycin at 37 °C and 5% $CO_2$. Stable CMV-EGR-1 and dnEGR-1 were selected using G418 sulfate (400 μg/ml). 22Rv1 cells were infected with Ad5/GFP (referred as Ad-GFP), Ad5/GFP-EGR-1 (referred as Ad-EGR-1) and Ad5/GFP-NAB1 (referred as Ad-NAB1) at a viral titer of $1 \times 10^8$ plaque-forming units/ml for 2 h.

*DNA transfection and CAT assays*
Stable transfections were performed using Lipofectamine plus reagent (Gibco BRL, Carlsbad, CA, USA). Transient transfections were performed by the calcium phosphate co-precipitation method or by effectene transfection reagent (Qiagen, Valencia, CA, USA). CAT assays were performed as described earlier (Ahmed *et al*., 1997).

*Irradiation*
A 100 kV industrial X-ray machine (Phillips, Amsterdam, The Netherlands) was used to irradiate the cultures. The dose rate with a 2-mm aluminum plus 1-mm beryllium filter was 2.64 Gy/min at a focus-surface distance of 10 cm.

*Colony-forming assay*
Prostate carcinoma, DU145 and 22Rv1 cells, transiently or stably transfected or infected cells were either left untreated or treated with 1–6 Gy. Stably transfected or infected DU145 and 22Rv1 cells were treated with 5 Gy. PC3 cells were left untreated or treated with 2 Gy radiation.

*EBS-GFP reporter assay*
PC3 cells transfected with EBS-GFP and EGR-1-WT or EGR-1-Y240A or EGR-1-Y235,240A or empty vector were either untreated or irradiated with 5 Gy dose, and the expression of GFP was observed 24 h later using Zeiss Axiovert 35 fluorescent microscope. The percentage of GFP-positive cells was determined.

*Quantitation of apoptosis*
Apoptosis was quantified by TUNEL staining and flow cytometry. The ApopTag *in situ* apoptosis detection kit (Oncor, Gaithersburg, MD, USA) was used for apoptosis as described earlier (Ahmed *et al*., 1997). To determine the percentage of cells showing apoptosis, approximately 1000 cells were counted in each of the four experiments performed. For flow cytometry, cells were dissociated using non-enzymatic cell dissociation medium (Sigma, St Louis, MO, USA), washed with phosphate-buffered saline, stained with Hoechst (Ho342) and merocyanine (MC540) and analyzed by flow cytometry using a FACStar Plus cell sorter (Ahmed *et al*., 1997).

*Cytochrome C release assay*
The 22Rv1 cells were infected with Ad-GFP, Ad-EGR-1 or Ad-NAB1 as described in earlier section for 24 h. The infected cells were then irradiated with 5 Gy. Post-irradiated cells (at 3 and 6 h) were then fractionated for mitochondrial and cytosolic fractions using a kit and instructions (BioVision, Mountain view, CA, USA). After protein estimation using Bradford's dye, samples were prepared for Western immunoblot analysis.

*Western blot analysis*
Total protein extracts from untreated and irradiated cells at various time intervals were subjected to western blot analysis using rabbit anti-EGR-1 (Santa Cruz Biotechnology, Santa Cruz, CA, USA), rabbit anti-Bax (Santa Cruz Biotechnology), rabbit anti-Bcl-2 (Santa Cruz Biotechnology), mouse anti-caspase 3 (Sigma, St Louis, MO, USA), mouse anti-PARP antibody (Sigma), rabbit anti-GRP75 (mitochondrial matrix-specific protein) (Santa Cruz Biotechnology), mouse anti-cytochrome *c* (BioVision) and mouse anti-β-actin antibody (Sigma). Secondary goat anti-mouse IgG and anti-rabbit IgG (Amersham, Piscataway, NJ, USA). The bound immune complexes were detected using chemiluminescence method.

*Colorimetric assay for caspases 3 and 9 activities*
Activity of caspases 3 and 9 were assayed colorimetrically using DEVD-pNA and LEHD-pNA substrates, respectively. Briefly, untreated and irradiated DU145-transfected cells were lysed in 50 μl of chilled Cell Lysis Buffer (BioVision, Mountain View, CA, USA) and incubated on ice for 10 min. The suspension was centrifuged for 1 min at 10 000 *g* and supernate (50 μl) was incubated with 50 μl of 2 × reaction buffer and 5 μl of 4 mM LEHD-pNA or DEVD-pNA for 1 h at 37 °C. The activity was measured at 405 nm, and the specific activity of the caspases was calculated using the molar extinction coefficient of pNA (8800/M/cm).

*Electrophoretic mobility shift assay*
Electrophoretic mobility shift assay was performed using Nushift kit (Geneka Biotechnology, Montreal, Quebec, Canada) and nuclear lysates from untreated and irradiated DU145 cells. The consensus oligo probe that contains Egr-1-binding site (underlined) is 5′-GGATCCAGCGGGGGC GAGCGGGGGCGAACG-3′. For supershift experiments, rabbit EGR-1 polyclonal antibody was incubated with binding buffer and nuclear extract for 20 min at 10 °C prior to adding oligo probe. Binding reactions were electrophoresed on a 5% polyacrylamide gel in 1 × Tris-glycine electrophoresis buffer.

*Generation of WW, SH3, Tudor domain protein array, peptide synthesis and labeling*
GST fusion proteins harboring the listed WW, SH3 and Tudor domains were arrayed (Espejo and Bedford, 2004). The following peptides encompassing the PPxY motif from EGR-1 and its mutants conjugated to biotin label were synthesized

(Biosynthesis Inc., Lewisville, TX, USA): biotin-TALQYP**PPAY**PAAK, biotin-TALQAP**PPAY**PAAK and biotin-TALQAP**PPAA**PAAK. Biotinylated peptides (10 attogram) were labeled as described earlier (Espejo and Bedford, 2004). A GenePix 4200A scanner (Axon Inc., Sunnyvale, CA, USA) was used for array analysis.

*Reciprocal co-immunoprecipitation of EGR-1 and YAP-1*
PC3 cell (80% confluent) lysates in RIPA buffer were incubated with protein A beads to preclear the lysate, which was incubated with anti-EGR-1, -YAP-1 or nonspecific rabbit IgG (at the ratio of 1:500 of IgG to precleared lysate) followed by incubation with protein A beads for 4 h at 4 °C. The beads were washed with RIPA buffer followed by washes with 62.5 mM Tris-HCl (pH 6.8). Elution was performed by adding SDS–polyacrylamide gel electrophoresis sample buffer and boiling at 95 °C for 1 min.

*Chromatin immunoprecipitation*
Chromatin immunoprecipitation assay was described earlier (Shareef *et al*., 2007) using $2–5 \times 10^9$ PC3 cells. PCR was performed using specific primers for BAX promoter (5′-GCCTGGGCAACACAGTGAG-3′ and 5′-GCTCCCTCGGGAGGTTTG-3′) that yielded ~500 bp product. HG6PD gene served as a negative control.

*Isolation of RNA and reverse transcriptase-PCR*
Total RNA extracted using TRIZOL reagent (Life Technologies, Foster City, CA, USA) was reverse-transcribed into cDNA. Specific primers for BAX gene (5′-CCAGCTCTGAGCAGATCATGAAG-3′ and 5′-GCAATCATCCTCTGCAGCTCCAT-3′) were used for reverse transcriptase-PCR. Primers for GAPDH gene were used as internal controls.

*PC-3 xenografts*
Pathogen-free athymic Balb/c nude mice (6–8 weeks old; Harlan Sprague Dawley, Indianapolis, IN, USA), which were handled according to the guidelines stipulated in '*Guide for the care and use of laboratory animals*' (DHHS publication NIH-85-23), were used. PC3 cells ($5 \times 10^6$) were injected subcutaneously on the medial side of thigh just above the stifle. The injected animals were monitored twice a week for subcutaneous tumors till the tumor volume reached at least 0.5 $cm^3$, when the animals were randomized into six groups. The tumor volumes were calculated by the Attria and Weiss formula: $a^2 \times b^2 \times 0.4$, where '*a*' is the smallest and '*b*' the largest tumor diameter (measured by calipers). Group I—parental xenografts, no treatment; group II—parental xenografts, 20 Gy of total IR dose; group III—Ad/GFP-treated xenografts; group IV—Ad/GFP-EGR-1-treated xenografts; group V—Ad/GFP-treated xenografts with 20 Gy total dose of IR; and group VI—Ad/GFP-EGR-1-treated xenografts with 20 Gy total dose of IR. Ad/GFP or Ad/GFP-EGR-1 constructs were injected into the tumor at a dose of 100 MOI (multiplicity of infection) ($3 \times 10^8$ PFU) at the first day of treatment followed by 2 Gy radiation dose per day to the tumor for 5 days. On 7th and 8th days, intra-tumoral injections of Ad/GFP or Ad/GFP-EGR-1 constructs were repeated followed by 2 Gy dose of radiation for 5 days. On the 14th day, the animals received the final 100 MOI of Ad/GFP or Ad/GFP-EGR-1 and were observed for next 7 weeks.

*PC-3 xenografts and tissue harvest for paraffin embedding*
Tissue, of one mice from each group euthanized on the 1st, 7th, 14th, 21st, 28th, 35th and 40th day of treatment, was fixed in 5% buffered formalin and embedded in paraffin. Paraffin sections were subjected to Bax immunohistochemistry using the avidin–biotin–peroxidase complex method.

*Statistical analysis*
For *in vitro* experiments, simple *t*-test was used. Animal groups were compared using the two-tailed Fisher's exact test.

## Acknowledgements

This work was supported by grants, NIH (RO1 CA78471), PCRP-DOD (PC 970526) and Charlotte Geyer foundation to MMA; post-doctoral training grant, PCRP-DOD (WB1XWH-04-1-0039) to MZ; NIH (DK62345) and Pennsylvania Department of Health Grant (SAP4100037378) to MMS and Welch Foundation Grant (G-1495) to MTB.

## References

Abdulkadir SA, Carbone JM, Naughton CK, Humphrey PA, Catalona WJ, Milbrandt J. (2001a). Frequent and early loss of the EGR1 corepressor NAB2 in human prostate carcinoma. *Hum Pathol* **32**: 935–939.

Abdulkadir SA, Qu Z, Garabedian E, Song SK, Peters TJ, Svaren J *et al*. (2001b). Impaired prostate tumorigenesis in Egr1-deficient mice. *Nat Med* **7**: 101–107.

Ahmed MM, Sells SF, Venkatasubbarao K, Fruitwala SM, Muthukkumar S, Harp C *et al*. (1997). Ionizing radiation-inducible apoptosis in the absence of p53 linked to transcription factor EGR-1. *J Biol Chem* **272**: 33056–33061.

Ahmed MM, Venkatasubbarao K, Fruitwala SM, Muthukkumar S, Wood Jr DP, Sells SF *et al*. (1996). EGR-1 induction is required for maximal radiosensitivity in A375-C6 melanoma cells. *J Biol Chem* **271**: 29231–29237.

Antonsson B, Montessuit S, Sanchez B, Martinou JC. (2001) Bax is present as a high molecular weight oligomer/complex in the mitochondrial membrane of apoptotic cells. *J Biol Chem* **276**: 11615–11623.

Basu S, Totty NF, Irwin MS, Sudol M, Downward J. (2003). Akt phosphorylates the Yes-associated protein, YAP, to induce interaction with 14-3-3 and attenuation of p73-mediated apoptosis. *Mol Cell* **11**: 11–23.

Buttyan R, Zakeri Z, Lockshin R, Wolgemuth D. (1988). Cascade induction of c-fos, c-myc, and heat shock 70K transcripts during regression of the rat ventral prostate gland. *Mol Endocrinol* **2**: 650–657.

Das A, Chendil D, Dey S, Mohiuddin M, Mohiuddin M, Milbrandt J *et al*. (2001). Ionizing radiation down-regulates p53 protein in primary Egr-$1^{-/-}$ mouse embryonic fibroblast cells causing enhanced resistance to apoptosis. *J Biol Chem* **276**: 3279–3286.

Datta R, Rubin E, Sukhatme V, Qureshi S, Hallahan D, Weichselbaum RR *et al*. (1992). Ionizing radiation activates transcription of the EGR1 gene via CArG elements. *Proc Natl Acad Sci USA* **89**: 10149–10153.

Day ML, Wu S, Basler JW. (1993). Prostatic nerve growth factor inducible A gene binds a novel element in the retinoblastoma gene promoter. *Cancer Res* **53**: 5597–5599.

Dong J, Feldmann G, Huang J, Wu S, Zhang N, Comerford SA *et al*. (2007). Elucidation of a universal size-control mechanism in *Drosophila* and mammals. *Cell* **130**: 1120–1133.

Eid MA, Kumar MV, Iczkowski KA, Bostwick DG, Tindall DJ. (1998). Expression of early growth response genes in human prostate cancer. *Cancer Res* **58**: 2461–2468.

Espejo A, Bedford MT. (2004). Protein-domain microarrays. *Methods Mol Biol* **264**: 173–181.

Kalkhoven E. (2004). CBP and p300: HATs for different occasions. *Biochem Pharmacol* **68**: 1145–1155.

Kyprianou N. (1994). Apoptosis: therapeutic significance in the treatment of androgen-dependent and androgen-independent prostate cancer. *World J Urol* **12**: 299–303.

Lee JM, Bernstein A. (1993). p53 mutations increase resistance to ionizing radiation. *Proc Natl Acad Sci USA* **90**: 5742–5746.

Macias MJ, Wiesner S, Sudol M. (2002). WW and SH3 domains, two different scaffolds to recognize proline-rich ligands. *FEBS Lett* **513**: 30–37.

Matallanas D, Romano D, Yee K, Meissl K, Kucerova L, Piazzolla D *et al*. (2007). RASSF1A elicits apoptosis through an MST2 pathway directing proapoptotic transcription by the p73 tumor suppressor protein. *Mol Cell* **27**: 962–975.

Matheny C, Day ML, Milbrandt J. (1994). The nuclear localization signal of NGFI-A is located within the zinc finger DNA binding domain. *J Biol Chem* **269**: 8176–8181.

Nair P, Muthukkumar S, Sells SF, Han SS, Sukhatme VP, Rangnekar VM. (1997). Early growth response-1-dependent apoptosis is mediated by p53. *J Biol Chem* **272**: 20131–20138.

Oka T, Mazack V, Sudol M. (2008). Mst2 and Lats kinases regulate apoptotic function of Yes kinase-associated protein (YAP). *J Biol Chem* **283**: 27534–27546.

Shareef MM, Cui N, Burikhanov R, Gupta S, Satishkumar S, Shajahan S *et al*. (2007). Role of tumor necrosis factor-alpha and TRAIL in high-dose radiation-induced bystander signaling in lung adenocarcinoma. *Cancer Res* **67**: 11811–11820.

Strano S, Blandino G. (2007). YAP1 meets tumor suppression. *Mol Cell* **27**: 863–864.

Sudol M. (1994). Yes-associated protein (YAP65) is a proline-rich phosphoprotein that binds to the SH3 domain of the Yes proto-oncogene product. *Oncogene* **9**: 2145–2152.

Sudol M, Bork P, Einbond A, Kastury K, Druck T, Negrini M *et al*. (1995). Characterization of the mammalian YAP (Yes-associated protein) gene and its role in defining a novel protein module, the WW domain. *J Biol Chem* **270**: 14733–14741.

Svaren J, Ehrig T, Abdulkadir SA, Ehrengruber MU, Watson MA, Milbrandt J. (2000). EGR1 target genes in prostate carcinoma cells identified by microarray analysis. *J Biol Chem* **275**: 38524–38531.

Tsujimoto Y. (1998). Role of Bcl-2 family proteins in apoptosis: apoptosomes or mitochondria? *Genes Cells* **3**: 697–707.

Virolle T, Adamson ED, Baron V, Birle D, Mercola D, Mustelin T *et al*. (2001). The Egr-1 transcription factor directly activates PTEN during irradiation-induced signalling. *Nat Cell Biol* **3**: 1124–1128.

Zender L, Spector MS, Xue W, Flemming P, Cordon-Cardo C, Silke J *et al*. (2006). Identification and validation of oncogenes in liver cancer using an integrative oncogenomic approach. *Cell* **125**: 1253–1267.

Supplementary Information accompanies the paper on the Oncogene website (http://www.nature.com/onc)